Dynamic Analysis of a Deployable Space Structure

G.E. Weeks*
The University of Alabama, Tuscaloosa, Alabama

A mathematical model and a corresponding simulation code have been developed for investigating the free-vibration and forced-response behavior of a deployable space structure. Specifically, the structure considered was the NASA Solar Array Flight Experiment configuration (that has undergone testing on a recent Shuttle flight) where the mast was modeled as an Euler beam column and the solar array was modeled as a membrane. The resulting partial differential equations of motion were transformed such that the boundary conditions were time-invariant. Subsequent use of the Galerkin method resulted in an infinite set of second-order differential equations that were truncated and solved for the frequency and forced-response behavior of the coupled structural components. It is demonstrated that accurate results for frequency and mode-shape characteristics can be obtained with only a small number of generalized coordinates and, thus, appears to be a more computationally efficient algorithm than the finite element method for this type of structure. Similarly, the truncated set of equations was numerically integrated to obtain response histories of certain pertinent variables from a packaged structure, through full deployment, to complete retraction.

Nomenclature

a_1 = center of gravity offset of mast tip
e_1 = distance from mast ℄ to array
EI = bending stiffness of mast
K_T = stiffness at mast-canister interface
L = instantaneous length of mast
M = mast bending moment
$\bar{M}$ = mast of mast tip fitting
P = compressive load in mast
t = time
T = tensile load in the solar array
V = mast transverse shear force
w,y = transverse deflection of solar array and mast, respectively
z = axial coordinate of SAFE structure

Introduction

STRUCTURAL configurations capable of being packaged into a small volume to be deployed on orbit to full size have been utilized on a number of well-known space-related activities over the past few years. However, immediate and future applications of the packaged-structure concept to structures with truly large-scale deployed dimensions, such as satellite solar arrays of sufficient size for commercial use and expandable component sections for the structural foundation of a permanent manned space station, present new and challenging structural, kinematics, and controls problems that must be considered.

In particular, this paper addresses the problem of the formulation and corresponding analysis of the dynamic response behavior for a packaged structure during the deployment modes of extension and/or retraction. The solutions of this problem present considerable mathematical difficulties mainly because the formulation results in partial differential equations of motion with time-variable coefficients and boundary conditions which are functions of time. Similar problems with nonstationary boundary conditions have been studied in ablation,[1] moving threadline,[2] and bandsaw motion.[3] However, the first work on a more directly related structural configuration appears to have been published by Worley,[4] where he studied the response behavior of a uniform Euler beam with a constant deployment speed. Since then a number of studies have been carried out on the deployable flexible appendage problem.[5-7] The objective of this study is to provide an efficient method of analysis for simulating the dynamic response behavior of a coupled structure that models a deployable appendage with an attached solar array blanket.

The formulation of the equations of motion for such a deployable structure and a corresponding simulation of its response behavior during deployment will obviously be a function of the geometry of the specific structure being considered. For this investigation, the deployable structure considered was the NASA SAFE (Solar Array Flight Experiment) configuration shown in Fig. 1, where a fiberglass, three-longeron, truss-type appendage initially coiled in a containment canister is connected to a packaged solar array blanket as indicated. Extension or retraction of this coupled structure is accomplished by means of a rotatable nut assembly driven by a constant-speed drive motor as shown in Fig. 2.

This particular configuration was chosen for consideration mainly because an actual prototype structure has been constructed and limited analytical and experimental data are available for validation of the mathematical model and solution algorithm to be presented in this study. Specifically, the SAFE structure has been analyzed to determine its natural frequencies and mode shapes at 70 and 100% deployment[8] using the SPAR[9] finite element code. Conceptually, this code or other general-purpose finite element codes (e.g., NASTRAN) could also be used for the direct integration of the equations of motion to trace accurately the response histories of displacement and stress at critical points in the structure during deployment. However, the finite element method typically requires several hundred degrees of freedom to model the structure accurately, which in turn requires the solution of these several hundred coupled equations of motion at each time step. When it is considered that several hundred to several thousand time steps are typically required to trace the response history of a complex structure accurately, it is apparent that significant amounts of computer time and expense could be required for dynamic analysis using the finite element method.

An alternate method of analysis is to model the structure with analytic functions defining its modal behavior. (It is

Submitted Feb. 6, 1985; presented as Paper 85-593 at the AIAA/ASME/ASCE/AHS 26th Structures, Structural Dynamics and Materials Conference, Orlando, FL, April 15-17, 1985; revision received May 16, 1985. This paper is declared a work of the U.S. Government and therefore is in the public domain.

*Professor of Aerospace Engineering.

pointed out that the classical procedure of modal superposition is not applicable for this investigation because of the time-varying stiffness of the structure during deployment/retraction.) The advantages of this approach are that, when applicable, accurate vibration and dynamic response histories can be obtained with a relative few degrees of freedom as compared to the finite element method. While this method of analysis is presented herein for investigation of the deployable dynamics of the SAFE structure, the basic procedure can be used for structures with different geometries, e.g., parabolic reflectors.

In order to focus attention on the development of the mathematical model, temporal operator considerations, and the effect of system parameters on dynamic response, this study will consider only the in-plane response of the SAFE structure. Extensional and torsional vibrations are neglected. The mathematical model is developed by integrating the equations of motion of the component elements, by parts, to establish a virtual work principle. Analytic functions defining the modal behavior of these component elements are then used with Galerkin's method to reduce the partial differential equations of motion to an infinite set of ordinary second-order differential equations with variable coefficients. A truncated set of these equations is then solved for the frequency and forced response behavior of the coupled structure. It is demonstrated that accurate results are obtained using only a small number of generalized coordinates.

Structural Model—Equations of Motion

The SAFE structure shown in Fig. 1 is ideally modeled as shown in Fig. 3 where the deployable mast is modeled as an Euler beam column of constant cross section and the solar blanket is modeled as a membrane. The corresponding equations of motion are

$$EIy''''(z,t) + [P(t)y'(z,t)]' + \rho_m \ddot{y}(z,t) = 0 \tag{1}$$

$$[T(t)w'(z,t)]' - \rho_b w(z,t) = 0 \tag{2}$$

where primes denote differentiation with respect to z and dots denote differentiation with respect to time. Multiplying Eq. (1) by $\delta y(z,t)$, Eq. (2) by $\delta w(z,t)$, integrating by parts over the instantaneous deployed length of the structure, and making use of the relations

$$w(L,t) = y(L,t) = 0 \tag{3}$$

$$M(L,t) = EIy''(L,t) = -K_T y'(L,t) \tag{4}$$

$$M(0,t) = EIy''(0,t) \tag{5}$$

$$V(0,t) = EIy'''(0,t) + P(t)y'(0,t) \tag{6}$$

result in the virtual work statement of the problem to be

$$\begin{aligned} &-Tw'(0,t)\delta w(0,t) + V(0,t)\delta y(0,t) \\ &-K_T y'(L,t)\delta y'(L,t) \\ &-M(0,t)\delta y'(0,t) + \int_0^{L(t)} [-\rho_b \ddot{w}(z,t)\delta w(z,t) \\ &-Tw'(z,t)\delta w'(z,t)]\,dz + \int_0^{L(t)} [-\rho_m \ddot{y}(z,t)\delta y(z,t) \\ &-EIy''(z,t)\delta y''(z,t) + Py'(z,t)\delta y'(z,t)]\,dz = 0 \end{aligned} \tag{7}$$

Explicit relations for $M(0,t)$, $V(0,t)$, and $P(t)$, in terms of the system coordinates, are obtained from the equations of motion of the rigid mast-tip fitting as shown in Fig. 4. These equations also couple the response of the mast and blanket.

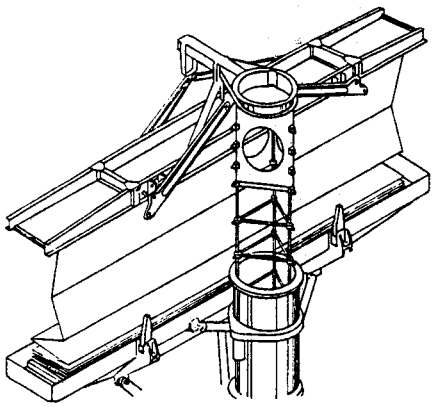

Fig. 1 SAFE configuration.

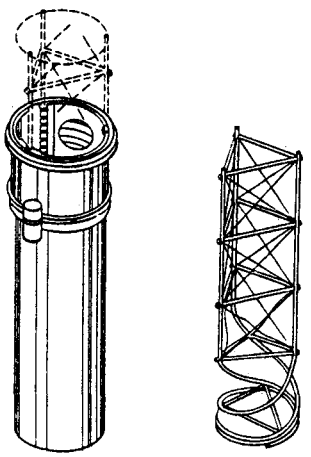

Fig. 2 Rotating nut assembly.

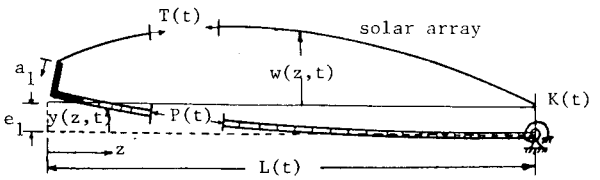

Fig. 3 Two-dimensional model, SAFE structure.

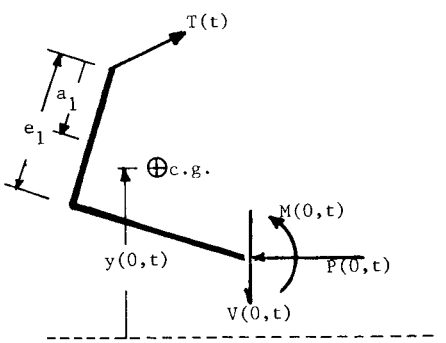

Fig. 4 FBD (Free Body Diagram)—mast tip fitting.

Neglecting higher order terms, the results are

$$M(0,t) = T(t)e_1 + (e_1 - a_1)\bar{M}\ddot{L}(t) \tag{8}$$

$$P(t) = T(t) + \bar{M}\ddot{L} \tag{9}$$

$$V(0,t) = T(t)w'(0,t) - \bar{M}\ddot{y}(0,t) \tag{10}$$

Note $\ddot{L}(t)$ is positive for extension and negative for retraction.

Considerable savings in computation time can be realized by transforming Eqs. (7-10) into a form such that the boundary conditions are not a function of time. This is accomplished by the transformation

$$x(t) = z(t)/L(t) \tag{11}$$

such that the mast and blanket boundaries are transformed from $z=0$, $L(t)$ to $x=0,1$. The derivatives with respect to z and t in Eqs. (7-10) then become

$$(\,)' = \frac{1}{L(t)}\frac{\partial(\,)}{\partial x}$$

$$(\,)'' = \frac{1}{L^2(t)}\frac{\partial^2(\,)}{\partial x^2}$$

$$(\ddot{}) = \frac{\partial^2(\,)}{\partial t^2} - \frac{2\dot{L}(t)}{L(t)} \times \frac{\partial^2(\,)}{\partial x \partial t} + \left[-\frac{\ddot{L}(t)}{L(t)} + \frac{2\dot{L}^2(t)}{L^2(t)}\right]\frac{\partial(\,)}{\partial x} + x^2\frac{\dot{L}^2(t)}{L^2(t)}\frac{\partial^2(\,)}{\partial x^2} \tag{12}$$

The final form of the equations of motion is derived by considering a series expansion of the mast and blanket displacements in the form

$$y(x,t) = \sum_{n=0}^{\infty} A_n(t)\,Y_n(x) \tag{13}$$

$$w(x,t) = \sum_{n=0}^{\infty} B_n(t)\,W_n(x) + \sum_{n=0}^{\infty} A_n(t)\,Y_n(0)(1-x) \tag{14}$$

where

$$W_n(x) = \sin n\pi x \tag{15}$$

and $Y_n(x)$ is the nth eigenfunction of a free rotationally restrained beam of fixed unit length. (The eigenfunctions and corresponding eigenvalues for this beam with a specified stiffness are presented in Appendix A.) Substituting Eqs. (13-15) into Eq. (7) [after making use of Eqs. (8-12)] and performing the indicated operations result in the following infinite set of second-order differential equations with variable coefficients:

$$\begin{bmatrix} \underset{\sim}{M}_{11}^{mn} & \underset{\sim}{M}_{12}^{mn} \\ \underset{\sim}{M}_{21}^{mn} & \underset{\sim}{M}_{22}^{mn} \end{bmatrix}\begin{bmatrix} \ddot{\underset{\sim}{A}}^n \\ \ddot{\underset{\sim}{B}}^n \end{bmatrix} + \begin{bmatrix} \underset{\sim}{C}_{11}^{mn} & \underset{\sim}{C}_{12}^{mn} \\ \underset{\sim}{C}_{21}^{mn} & \underset{\sim}{C}_{22}^{mn} \end{bmatrix}\begin{bmatrix} \dot{\underset{\sim}{A}}^n \\ \dot{\underset{\sim}{B}}^n \end{bmatrix} + \begin{bmatrix} \underset{\sim}{K}_{11}^{mn} & \underset{\sim}{K}_{12}^{mn} \\ \underset{\sim}{K}_{21}^{mn} & \underset{\sim}{K}_{22}^{mn} \end{bmatrix}\begin{bmatrix} \underset{\sim}{A}^n \\ \underset{\sim}{B}^n \end{bmatrix} = \begin{bmatrix} \underset{\sim}{F}_1^m \\ \underset{\sim}{F}_2^m \end{bmatrix} \tag{16}$$

where the matrix coefficients M_{ij}^{mn}, C_{ij}^{mn}, K_{ij}^{mn}, and F_j^m are listed in Appendix B. It is noted that if the deployment velocity and accelerations are zero, the pseudodamping matrix vanishes and the resulting equations are coupled through the mass matrix only.

The deployable dynamic behavior of the SAFE structure is now obtained by numerically integrating Eq. (16), subject to specified initial conditions, and substituting the results into Eqs. (13) and (14) to evaluate the response histories of the mast and solar array. A discussion of the method of integration used in this study is presented in the next section.

Numerical Solution Procedure—Temporal Operator Considerations

For structural systems with no coupled damping, modal-superposition techniques are typically utilized to obtain response histories by transforming the equations of motion into principal coordinates and solving the resulting set of uncoupled equations. However, for the deploying structure, not only does this coupled damping occur, but the mass and stiffness matrices are continually changing with time. These considerations then preclude formulation of an uncoupled set of equations so that a direct step-by-step integration of the equations of motion [Eq. (16)] is required to determine the system response.

Numerous integration algorithms (or temporal operators) are available for carrying out this step-by-step integration; implicit and explicit schemes and single and multistep methods. The ideal operator would be easy to implement, unconditionally stable, and exhibit no artificial attenuation of the amplitude and phase response for any reasonable time step chosen. No such operator exists and although significant effort has been devoted to the development of such computationally efficient algorithms[10-12] in recent years with some success, the constant-average-acceleration version for the Newmark operator[13] and the Wilson-θ operator ($\theta = 1.4$)[14] are still considered to be the most appropriate even though each has recognized drawbacks for specific problems. Consequently, these two explicit operators were initially selected in this study for integrating the equations of motion of the deployable structure (the explicit schemes were not considered because of their typical numerical instability characteristic and extremely small step size required to trace the system response accurately). In general it was found that results obtained from the Newmark operator were unsatisfactory because of the magnitude of the spurious participation of the higher modes. On the other hand, the Wilson method appeared to produce acceptable response histories for all cases considered and, hence, was the temporal operator used for this study.

Finally, it is appropriate to point out a problem with any technique of numerical integration that is unique to deployable dynamics. A well-known rule of thumb used for step-by-step integration algorithms is that the time step used should be a certain fraction of the fundamental (or highest) period to trace the system response accurately. Now consider that from initial to final deployment, the fundamental frequency of a typical configuration may vary by an order of magnitude or more. Correspondingly, the time step required to trace the initial response will be similar orders of magnitude smaller than required toward the final stages of deployment. If the initial step size is kept constant throughout the deployment history excessive CPU time is required. Thus, it would appear that a variable time step consistent with the variation in frequency with deployed length would represent an optimum choice of step size, in terms of minimum required CPU time. However, the effect of a variable step size on temporal operator behavior—artificial attenuation and damping of spurious modes—does not appear to have been investigated in the literature.

Structural Response—Numerical Results

The SAFE deployment/retraction scenario is illustrated in Fig. 5. From package to 70% deployment, the array is stabilized by guy wires with a constant total tensile force of 4.8 lb. At 70%, a tension bar attached to the array is abruptly engaged to prestress the array with a tensile load of 11.75 lb, resulting in a total mast compressive force of 16.55 lb. After reaching quiescence, the SAFE is deployed from 70 to 100% with the constant mast compressive force of 16.55 lb. At

100%, a final bar is engaged that abruptly changes the mast compressive force from 16.55 to 23 lb.

Natural Frequencies and Mode Shapes

The basic stiffness, mass, and geometric parameters that define the SAFE structure are presented in Table 1. With these values, natural frequencies and mode shapes were computed from Eq. (16) using five beam modes for the mast [Eq. (13)] and five modes for the array [Eq. (15)]. The results for the first three in-plane frequencies of the structure at 70 and 100% deployment are shown in Table 2, along with results obtained using the finite element method.[8] Assuming the finite element results were exact, the results obtained from the present formulation, using only ten generalized coordinates, are in error by approximately 5% for the first natural frequency and less than 10% for the second and third frequencies—adequate accuracy for design. The mode shapes corresponding to the first two natural frequencies are shown in Fig. 6. Also, for completeness, the variation in the first two natural frequencies of the SAFE—as a function of deployed length—is shown in Fig. 7.

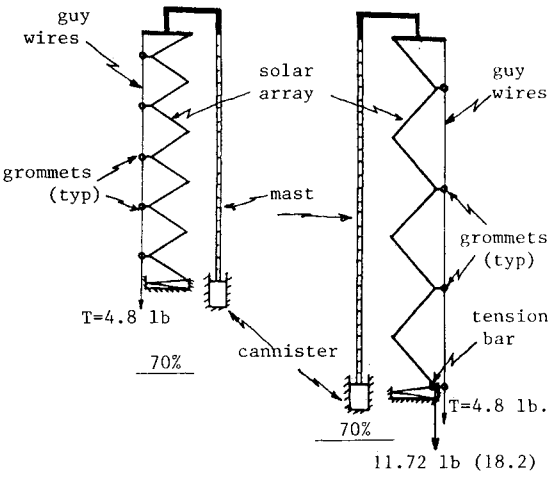

Fig. 5 SAFE deployment—stabilizing forces.

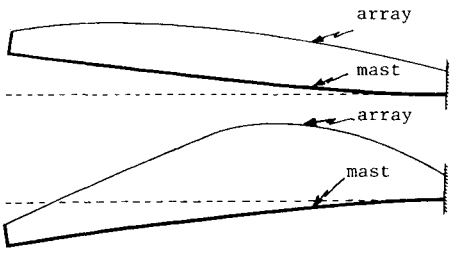

Fig. 6 SAFE—first two mode shapes.

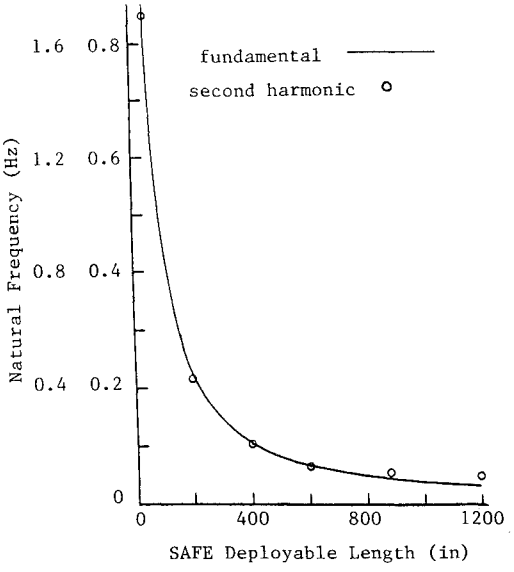

Fig. 7 Frequency variation with deployed length.

Dynamic Response

The equations of motion [Eq. (16)] were integrated numerically, using the Wilson-θ algorithm discussed previously, to obtain the SAFE response for various deployment/retraction scenarios. All results were obtained using five modes for the mast and blanket. As an aid in interpreting and verifying the dynamic response results presented subsequently, the mast tip static deflections, as a function of the applied load and deployment length, are shown in Table 3.

The mast tip displacement response from 0 to 70% deployment is shown in Fig. 8. Note that until the 70% length is attained, the small load (4.8 lb) and slow deployment speed (1.5 in./s) result in essentially static behavior with the tip deflection approaching the static equilibrium value of 1.27 in. At 70%, the structure is "hit" with an additional 11.75-lb step function load. Note that the oscillations are about the static equilibrium position fo 4.55 in. and an apparent beat phenomenon exists due to traveling waves.

The mast tip displacement response from 70 to 100% deployment is shown in Fig. 9, assuming the structure was initially at rest and then "hit" instantaneously with a 16.55-lb load. The tip initially oscillates about the static equilibrium position (4.55 in. at 70%), and during deployment to 100% the tip continues to oscillate about the variable static equilibrium position, reaching 9.57 in. at 100%. At 100%, the structure is "hit" with an additional 6.45-lb load resulting in oscillations about the new static position (14.05 in.). Note that changes in structural stiffness of the SAFE due to a change in length and axial loading are reflected in Fig. 9 by the changes in the vibration period during deployment.

Table 1 SAFE structural parameters

Mast weight, lb	41.6
Mast length (fully extended), in.	1260
Mast tip fitting (weight), lb	59
Mast tip c.g., a_1; in.	6.6
Array offset from mast ℄, e_1; in.	10.6
Mast stiffness, EI; lb-in.^{2}	18×10^6
Mast base compliance, K_T; in.-lb/rad	300,000
Mast deployment speed, in./s	1.5

Table 2 SAFE natural frequencies, Hz

		Mode		
		1	2	3
Present investigation	70%	0.058	0.108	0.179
	100%	0.036	0.092	0.145
Ref. 2	70%	0.059	0.119	0.196
	100%	0.034	0.096	0.153

Table 3 SAFE tip deflection under static loads

Deployed length, in.	Load, lb	Displacement, in.
70% = 882	4.8	1.27
	16.55	4.55
100% = 1260	16.55	9.57
	23.0	14.05

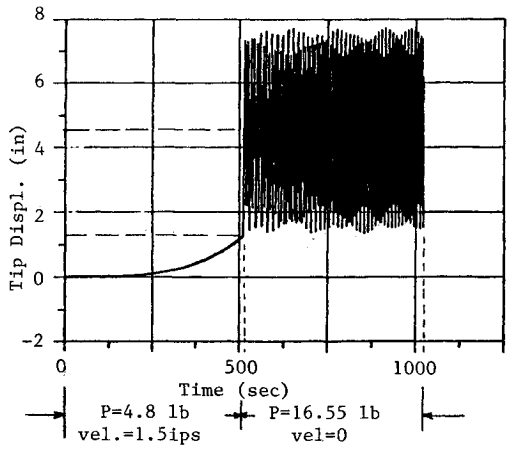

Fig. 8 Mast tip response history, 0-70% deployment.

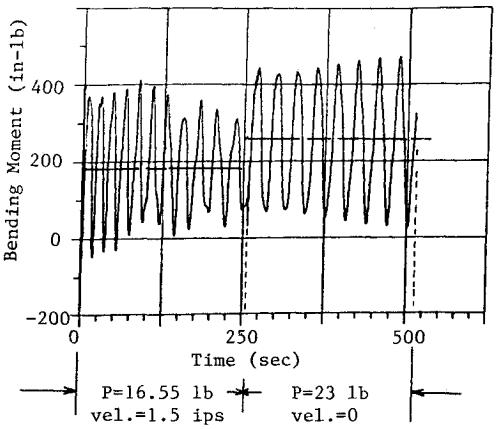

Fig. 11 Mast base moment, 70-100% deployment.

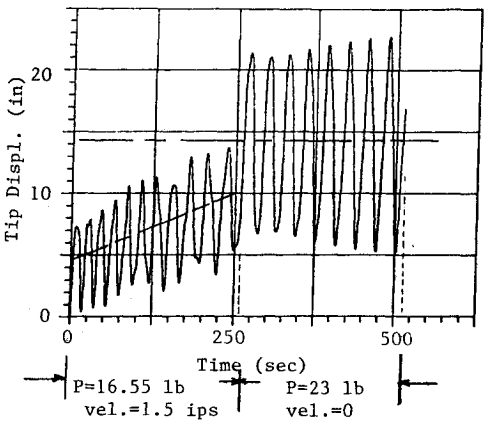

Fig. 9 Mast-tip displacement, 70-100% deployment.

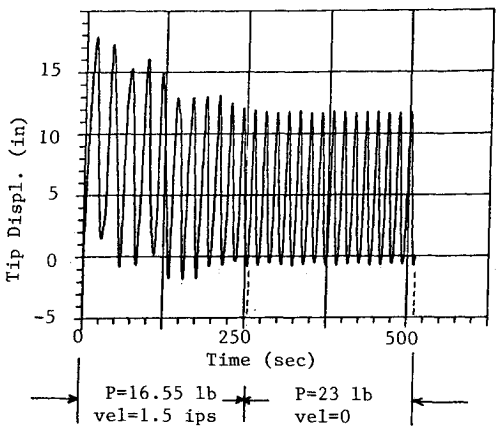

Fig. 12 Mast tip displacement, 100-70% retraction.

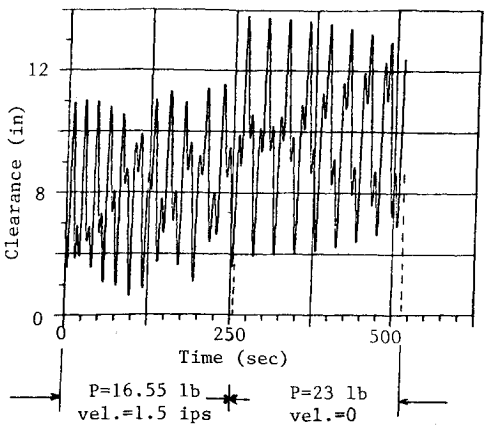

Fig. 10 Mast-array clearance, 70-100% deployment.

For the SAFE configuration in particular, a primary concern was the mast-array clearance during deployment. Figure 10 shows the results from this simulation for the net clearance between the mast and array (at the instantaneous mast-array midpoints) during the 70-100% deployment. It is noted that a positive clearance is maintained throughout deployment. For completeness, the mast base bending moment is shown in Fig. 11 for the 70-100% deployment scenario. From 70 to 100%, the bending moment response oscillates about the static equilibrium value ($10.6 \times 16.55 = 175.4$ in.-lb). At 100%, the additional load of 6.45 lb results in the moment oscillating about the new equilibrium value of $10.6 \times 23 = 243.8$ in.-lb. (The effect of deformed equilibrium positions on moment calculations was not included here for convenience.)

Finally, the mast tip response is shown in Fig. 12 for retraction from 100 to 70%. These results were obtained assuming the structure was initially "hit" with a 23-lb load for 0.01 s. Thereafter, a constant 16.55-lb load was applied until retraction to 70% was obtained. Comparing Figs. 9 and 12 indicates an important point that should be considered when dealing with deployable structures—the retraction behavior is not identical to the deployment behavior. In general, this is attributable to the fact that the natural frequencies of an expanding structure will be less than those of the same structure when retracting.

Conclusions

An efficient mathematical procedure and a corresponding simulation code have been developed for investigating the dynamic response behavior of a deployable space structure. Numerical results have been obtained for a particular configuration although the procedure is immediately applicable to any configuration typical of deployable structures. The method has been verified for natural frequency and mode-shape predictions by comparison with published results obtained using the finite element method. No published data are available for comparison with the computed response histories, although confidence in the methodology and results is justified by consideration of the magnitudes of these response histories with known values of static equilibrium configurations. Finally, the method of analysis presented here should be considered as a viable alternative to the finite element method of analysis for a large number of proposed deployable space structures because of the significantly re-

duced number of proposed deployable space structures because of the significantly reduced number of degrees of freedom required to obtain comparable accuracy.

Appendix A

The beam modes used in this analysis [Eq. (13)] correspond to a beam of unit length free at the left end and elastically restrained against rotation at the right end. With these conditions, the eigenvalues (natural frequencies) are given by solution of the equation

$$\sin\lambda_n\cosh\lambda_n-\cos\lambda_n\sinh\lambda_n-\frac{\gamma}{\lambda_n}(1+\cos\lambda_n\cosh\lambda_n)=0 \qquad \text{(A1)}$$

where

$$\lambda_n=\frac{mw_n^2}{EI}, \qquad \gamma=\frac{K_T}{EI} \qquad \text{(A2)}$$

and K_T is the stiffness (in.-lb/rad) at the mast-canister interface. The corresponding beam modes are given by the equation

$$Y_n(x)=\cosh\lambda_n x+\cos\lambda_n x-k_n(\sinh\lambda_n x+\sin\lambda_n x) \qquad \text{(A3)}$$

where

$$k_n=(\cosh\lambda_n+\cos\lambda_n)/(\sinh\lambda_n+\sin\lambda_n) \qquad \text{(A4)}$$

For the specific structure considered, $K_T=300{,}000$ in.-lb/rad and $EI=18{,}000{,}000$ lb-in.^{2}. The resulting first ten eigenvalues are

$\lambda_1=1.7947724$ $\lambda_6=16.859803$

$\lambda_2=4.5194452$ $\lambda_7=19.966843$

$\lambda_3=7.5950817$ $\lambda_8=23.079604$

$\lambda_4=10.670567$ $\lambda_9=26.196822$

$\lambda_5=13.760235$ $\lambda_{10}=29.317565$

Appendix B

The elements appearing in the mass, stiffness, and load matrices in Eq. (16) are given by the following expressions:

$$M_{11}=-\rho_b L Y_n(0)Y_m(0)\int_0^1(1-x^2)\mathrm{d}x$$
$$-\rho_m L\int_0^1 Y_n(x)Y_m(x)\mathrm{d}x-\bar{M}Y_n(0)Y_m(0)$$

$$M_{12}=M_{21}=-\rho_b L Y_m(0)\int_0^1 W_n(x)(1-x)\mathrm{d}x$$

$$M_{22}=-\rho_b L\int_0^1 W_n(x)W_m(x)\mathrm{d}x$$

$$C_{11}=-2\rho_b\dot{L}Y_n(0)Y_m(0)\int_0^1 x(1-x)\mathrm{d}x$$
$$+2\rho_m\dot{L}\int_0^1 xY_n'(x)Y_m(x)\mathrm{d}x$$

$$C_{12}=2\rho_b\dot{L}Y_m(0)\int_0^1 x(1-x)W_n'(x)\mathrm{d}x$$

$$C_{21}=-2\rho_b\dot{L}Y_n(0)\int_0^1 xW_m(x)\mathrm{d}x$$

$$C_{22}=2\rho_b\dot{L}\int_0^1 xW_n'(x)W_m(x)\mathrm{d}x$$

$$K_{11}=-\frac{K_T}{L^2}Y_n'(1)Y_m'(1)-\frac{T}{L}Y_n(0)Y_m(0)$$
$$-\frac{EI}{L^3}\int_0^1 Y_n''(x)Y_m''(x)\mathrm{d}x+\frac{T}{L}\int_0^1 Y_n'(x)Y_m'(x)\mathrm{d}x$$
$$+\rho_b\left(2\frac{\dot{L}^2}{L}-\ddot{L}\right)Y_n(0)Y_m(0)\int_0^1 x(1-x)\mathrm{d}x$$
$$+\frac{\bar{M}\ddot{L}}{L}\int_0^1 Y_n'(x)Y_m'(x)\mathrm{d}x+\rho\ddot{L}\int_0^1 xY_n'(x)Y_m'(x)\mathrm{d}x$$
$$-\rho_m\int_0^1\left[\frac{\dot{L}^2}{L}x^2Y_n''(x)+\left(2\frac{\dot{L}^2}{L}-\ddot{L}\right)xY_n'(x)\right]Y_m(x)\mathrm{d}x$$

$$K_{12}=-\rho_b\frac{\dot{L}^2}{L}Y_m(0)\int_0^1 x^2(1-x)\mathrm{d}x$$
$$-\rho_b\left(2\frac{\dot{L}^2}{L}\ddot{L}\right)Y_m(0)\int_0^1 x(1-x)W_n'(x)\mathrm{d}x$$

$$K_{21}=\rho_b\left(2\frac{\dot{L}^2}{L}-\ddot{L}\right)Y_n(0)\int_0^1 xW_m(x)\mathrm{d}x$$

$$K_{22}=-\frac{T}{L}\int_0^1 W_n'(x)W_m'(x)\mathrm{d}x$$
$$-\rho_b\frac{\dot{L}^2}{L}\int_0^1 x^2W_n''(x)W_m(x)\mathrm{d}x$$
$$-\rho_b\left(2\frac{\dot{L}^2}{L}-\ddot{L}\right)\int_0^1 xW_n'(x)W_m(x)\mathrm{d}x$$

Acknowledgments

The author would like to express his appreciation to Messrs. Dick Schock and Homer Pack of the NASA Marshall Space Flight Center for providing details of structural parameters, deployment scenarios, etc., of the SAFE structure.

References

[1]Boley, B.A., "Upper and Lower Bounds in Problems of Melting or Solidifying Slabs," *Quarterly Journal of Mechanics and Applied Mathematics,* Vol. 17, Pt. 3, 1964, p. 253.

[2]Swope, R.D. and Ames, W.F., "Vibration of a Moving Threadline," *Journal of the Franklin Institute,* Vol. 275, Jan. 1963, pp. 36-55.

[3]Mote, C.D., "A Study of Band-Saw Vibrations," *Journal of the Franklin Institute,* Vol. 279, No. 6, 1965, pp. 430-444.

[4]Worley, H.E., "Dynamic Response of Beams to Time-Varying Length," Ph.D. Dissertation, Department of Engineering Mechanics, The University of Alabama, Tuscaloosa, 1969.

[5]Tabarrok, B. et al., "On the Dynamics of an Axially Moving Beam," *Journal of the Franklin Institute,* Vol. 297, No. 3, 1974, pp. 201-220.

[6]England, F.E., "A Normal Mode Analysis of a Satellite Employing Long Flexible Booms," Ph.D. Dissertation, University of Maryland, College Park, 1969.

[7]Lips, K.W. and Modi, V.J., "Dynamics of a Deploying Orbiting Beam-Type Appendage Undergoing Vibration," *Journal of Vibration, Acoustics Stress, and Reliability in Design,* Vol. 105, Jan. 1983, pp. 33-39.

[8]Venator, T., "Updated Solar Array Flight Experiment Model," Lockheed Missiles and Space Co., Engineering Memo. DS/R-536, Sunnyvale, CA, April 5, 1983.

[9]"SPAR Structural Analysis System Reference Manual," NASA CR 158970-2, 1978.

[10]Argyris, J.H. et al., "Dynamic Response by Large Step Integration," *Earthquake Engineering and Structural Dynamics,* Vol. 2, Oct./Dec. 1973, pp. 185-203.

[11]Hilber, H.M. et al., "Improved Numerical Dissipation for Time Integration Algorithms in Structural Dynamics," *Earthquake Engineering and Structural Dynamics,"* Vol. 5, July/Sept. 1977, pp. 283-292.

[12]Kreg, R.D. and Key, S.W., "Transient Shell Response by Numerical Time Integration," *International Journal for Numerical Methods in Engineering,* Vol. 7, No. 3, 1973, pp. 273-286.

[13]Newmark, N.M., "A Method of Computation for Structural Dynamics," *Journal of the Engineering Mechanics Division, ASCE,* Vol . 85, EM3, July 1959, pp. 67-69.

[14]Bathe, K.J. and Wilson, E.L., "Stability and Accuracy Analysis of Direct Integration Methods," *Earthquake Engineering and Structural Dynamics,* Vol. 1, Jan./March 1973, p. 283.